REVIEWS

Journal of Semiconductors
(2021) 42, 081801
doi: 10.1088/1674-4926/42/8/081801

Ultraviolet communication technique and its application

Liang Guo[1, 2, 3], Yanan Guo[1, 2, 3], Junxi Wang[1, 2, 3], and Tongbo Wei[1, 2, 3, †]

[1]Research and Development Center for Semiconductor Lighting Technology, Institute of Semiconductors, Chinese Academy of Sciences, Beijing 100083, China

[2]Center of Materials Science and Optoelectronics Engineering, University of Chinese Academy of Sciences, Beijing 100049, China

[3]Beijing Engineering Research Center for the 3rd Generation Semiconductor Materials and Application, Beijing 100083, China

Abstract: With recent developments of deep ultraviolet (DUV) light-emitting diodes and solar-blind detectors, UV communication (UVC) shows great potential in replacing traditional wireless communication in more and more scenarios. Based on the atmospheric scattering of UV radiation, UVC has gained considerable attention due to its non-line-of-sight ability, omnidirectional communication links and low background noise. These advantages make UVC an ideal option for covert secure communication, especially for military communication. In this review, we present the history and working principle of UVC with a special focus on its light sources and detectors. Comprehensive comparison and application of its light sources and detectors are provided to the best of our knowledge. We further discuss the future application and outlook of UVC. Hopefully, this review will offer valuable insights into the future development of UVC.

Key words: ultraviolet communication; non-line-of-sight; optical wireless communication

Citation: L Guo, Y N Guo, J X Wang, and T B Wei, Ultraviolet communication technique and its application[J]. *J. Semicond.*, 2021, 42(8), 081801. http://doi.org/10.1088/1674-4926/42/8/081801

1. Introduction

Optical wireless communication (OWC) has been a research hot spot for decades[1]. From ultraviolet (UV) light to infrared (IR) light, OWC has been extensively studied. As the most popular optical communication technology, visible light communication (VLC) has received worldwide attention due to its over 10 Gb/s data rate and lower than 3.8×10^{-3} bit-error-rate (BER), which shows great potential in indoor high-speed communication[2]. The development of VLC has largely benefited from the development of light sources, especially visible light-emitting diodes (LEDs) technology. With the recent development of deep ultraviolet (DUV) LEDs and solar-blind detectors, ultraviolet communication (UVC) is drawing more and more attention too.

As a novel communication technique, UVC utilizes UV radiation to transmit signals which can be scattered and reflected by the particles and aerosols floating in the air. Its transmission range can be extended up to several kilometers regardless of the topographic features on the ground. Compared to traditional wireless communication, UVC has several unique features that render it a promising communication technique for future applications. Traditional wireless communication demands an obstacle-free communication channel between transceivers, while UVC can easily bypass these obstacles through scattering and reflection. The UV radiation employed in communication is also called solar-blind radiation which is located between 200–280 nm in the DUV spectrum. Most solar-blind radiation is absorbed by ozone and oxygen when passing through the atmosphere, which leaves a low background-noise communication channel near the ground[3]. Furthermore, the power of DUV radiation drops exponentially with the transmission distance, which limits its propagation and makes it an ideal option for short-range communication. In radio-silent scenarios, UVC can work as an alternative to conventional wireless communication. Fig. 1 shows an example of UVC system and network[4]. Recently, Alkhazragi *et al.* demonstrated a UVC system with a record-breaking data rate of 2.4 Gb/s. The proposed system was based on 279 nm LED and Si-based avalanche photodiode (APD), signaling that UVC has great potential in replacing traditional wireless communication in more and more scenarios.

In this article, we summarize and describe the history and working principle of UVC. A comprehensive comparison of its light sources and detectors is provided to the best of our knowledge. Then we discuss the research progress of UVC from a device perspective. For light sources, our review is based on three of the most used UV light sources including a gas discharge lamp, laser and LED. For detectors, other than the commonly-used detectors including photomultiplier tubes (PMTs) and semiconductor photodetectors (PDs), we also discuss some potential solar-blind detectors for UVC. Finally, we present the application and outlook of UVC. Hopefully, this review will offer valuable insights into the future development of UVC.

2. Development history of UVC

UVC was first put forward in the 1930s. Hulburt from the Naval Research Laboratory summarized their work from 1926 to 1933 in a report called "Signaling and Detection with Ultra-Violet and Infra-Red Radiation"[5]. They employed a 3 kW, 3 inch carbon arc searchlight equipped with a UV filter as light sources and a telescope with a fluorescent screen as detectors. The searchlight and telescope were accurately pointed towards each other to maximize the detection efficiency.

Correspondence to: T B Wei, tbwei@semi.ac.cn
Received 16 FEBRUARY 2021; Revised 29 MARCH 2021.

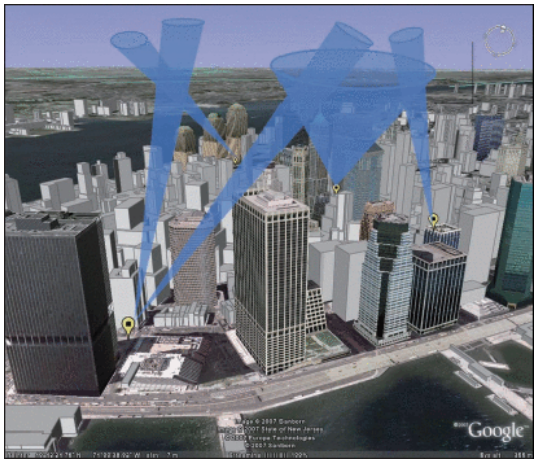

Fig. 1. (Color online) An example of UVC system and network[4].

They achieved a maximum transmission distance of 6 miles, but the communication system worked only at night. In 1945, White from University of California, Berkeley built a UVC prototype that achieved a maximum transmission distance of 3 miles, using a gallium arc lamp mounted on a 6-inch-diameter reflector as light sources, phosphor telescope and photomultiplier tube as detectors[6]. Sunstein *et al.* also systematically investigated the long-range UVC link in 1968[7]. A xenon flash tube and photomultiplier were used as the transmitter and receiver.

In 1994, Charles *et al.* first proposed solid-state lasers as the light sources for UVC. A compact quadrupled Nd:YAG laser was used to prove the feasibility[8]. The development of DUV LED promoted its application in UVC[3]. A source array composed of 240 research-graded 275 nm DUV LEDs with a total output power of 4.5 mW was used in UVC by Shaw *et al.*[9]. They achieved a 200 b/s link for node separations of up to 100 m.

The US Defense Advanced Research Projects Agency (DARPA) launched two programs involving developing novel light sources and detectors for future military use in 2002 and 2007: the Semiconductor UV Optical Source (SUVOS) program and the Deep Ultraviolet Avalanche Photodiode (DUVAP) program. These two programs sponsored numerous pieces of research on DUV light sources and solar-blind detectors, which further boosted the development of UVC based on DUV light sources and solar-blind detectors. In 2006, a 24-unit array LED with wavelength of 274 nm and output power of 40 mW was demonstrated by Shaw *et al.*[10]. They achieved a 2.4 Kb/s mixed-excitation linear predictive (MELP) vocoder link in full sunlight at a range of 11 m. Xu *et al.* and his team from the University of California (Riverside) conducted a series of experiments on system performance analysis, scattering model, modulate scheme and network communication since 2007. The research papers were also published continuously[4, 11–13].

UVC research in China was first started by the Beijing Institute of Technology in the 1990s[14]. Ni and his group built a short-distance voice communication UVC prototype using a low-pressure mercury lamp as the light source, and a PMT as the receiver[15]. In 2007, Tang *et al.* put forward a single scatter model that can effectively budget and evaluate the transmission distance of the non-line-of-sight (NLOS) UVC system in the solar-blind range. The model was successfully verified by the experiment results[16]. They further extended the application of this model to the evaluation of signal-noise ratio (SNR) and BER[17].

In 2009, researchers from Ben Gurion University in Israel developed an underwater UVC system based on 250 nm LED[18]. The system showed excellent communication performance. When transmission distance was over 170 m, the BER was lower than 10^{-4} and the data rate was 100 Mb/s. Researchers from Greece University conducted a series of experiments on path losses in the UVC system under different distances, elevation angles, and atmospheric conditions[19].

The National University of Defense Technology began the study on UVC in 2000. Jia *et al.* conducted several experiments on the scatter propagation model of the UV light based on the Monte Carlo method[20, 21]. They did extensive research on the influencing factors on the transmission range, data speed, and propagation characteristics of NLOS UVC links since 2011[22–25].

UVC research in Beijing University of Posts and Telecommunications started in 2010. Zuo *et al.* studied path loss in a novel single-scatter model based on Monte Carlo simulation[26]. They extended their research to propagation models under atmospheric turbulence in 2013[27, 28]. Guo *et al.* studied the spatial-division technology and the diversity reception algorithms in a UVC system[29]. In the same year, Meng *et al.* also demonstrated applied diversity reception technology to a real-time NLOS UVC system based on a 9.3 mW LED array[30]. The BER during the turbulence of the NLOS UVC system with On-Off Keying (OOK) modulation and Maximum Likelihood (ML) detection was analyzed and compared with that in free space without turbulence. In 2018, Sun *et al.* used a 266 nm DUV LED array with 50 mW luminous power as the light source achieving a high data rate of 921.6 Kb/s and BER of less than 10^{-7} in 150 m, which can beat the best record created by DUV LED communication system in terms of the data rate[31].

Studies at King Abdullah University of Science & Technology mainly focused on underwater UVC. Research based on laser and LED have been published successively[32, 33]. In 2018, He *et al.* from the University of Strathclyde in the UK achieved a record-high data rate of 1 Gb/s with 262 nm micro-LED[34]. The bandwidth of the light sources was 438 MHz at a current density of 71 A/cm^2 when saturating. In the same year, Kojima *et al.* from Tohoku University in Japan reported a 1.6 Gb/s error-free transmission over a 1.5 m line-of-sight (LOS) link in direct sunlight with a 280 nm LED[35].

3. Working principle of UVC

3.1. Configuration of UVC

A typical configuration of UVC is shown in Fig. 2. The transmitter side consists of the signal generator, current sources, modulation circuits and light sources such as DUV LEDs, DUV lasers, or mercury lamps. The electrical signals from the signal generator are coded by a modulation circuit and converted into high-frequency currents. Then high-frequency currents are amplified by current sources and supplied to light sources to generate light signals.

The receiver side consists of a solar-blind filter, UV detectors (usually PMT, p–i–n photodiode (PIN), or avalanche photodiode (APD)), signal amplifier, demodulator and so on. The

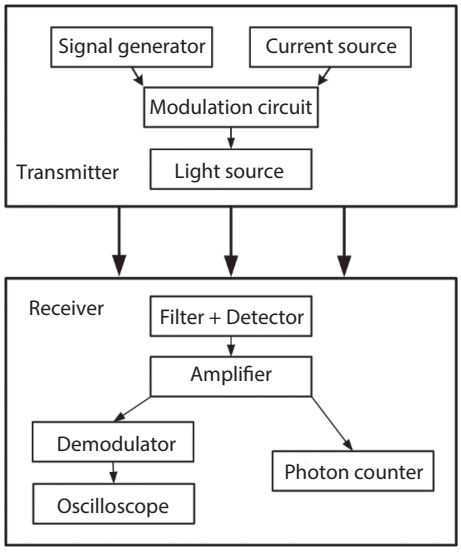

Fig. 2. The typical configuration of UVC.

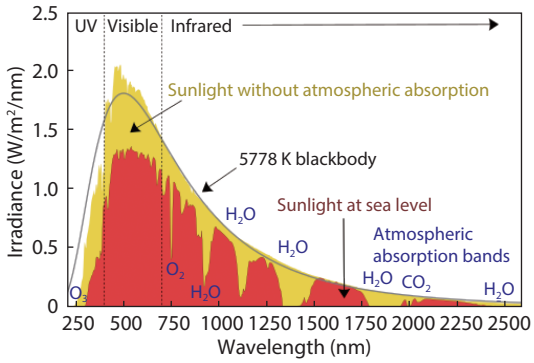

Fig. 3. (Color online) The spectrum of solar radiation on earth[37].

light signal detected by the UV detector will be converted back into the electrical signal. In order to increase the SNR, a signal amplifier is required to increase signal power. After demodulation and reconstruction, the signal will be restored.

3.2. Atmosphere propagation

When passing through the atmosphere, solar radiation is strongly scattered, absorbed, or reflected by the water vapor, carbon dioxide, fine particles, oxygen, ozone and other gas molecules in the air, causing discontinuities in the solar spectrum. Of all the molecules and particles, ozone which accounts for only 0.01%–0.1% of the atmosphere has a strong absorption band in the UV spectrum[36]. The UV part of solar radiation near the ground consists of about 95% UV-A and 5% UV-B; UV-C and most of UV-B are removed by stratospheric ozone. Fig. 3 shows that the distribution of the solar radiation spectrum near the ground.

Atmospheric scattering is the basis of NLOS UVC. When the light propagates in the atmosphere, its electromagnetic field will oscillate with the charges of particles floating in the air, which will generate one or more dipoles that radiate secondary spherical waves with the same frequency and phase as the original ones[38]. Generally, the closer the size of the particles is to the wavelength of UV light, the stronger the UV light will be scattered. Two scattering models are used in the study of scattering characteristics of UV radiation according to the relationship between the particle size and the light wavelength: Rayleigh scattering model and Mie scattering model.

Assuming that the intensity of monochromatic light radiation is I, the absorption caused by atmospheric scattering and absorption obeys the Lambert–Beer law[39]:

$$I = I_0 e^{-\mu(\lambda)l}. \tag{1}$$

I_0 is the luminous flux before absorption, I is the luminous flux after absorption, l is the transmission distance and $\mu(\lambda)$ is the light's atmospheric attenuation coefficient of the wavelength of λ per distance unit. Atmospheric attenuation coefficient can be derived from the following expression:

$$\mu(\lambda) = \alpha_a(\lambda) + \alpha_m(\lambda) + \beta_a(\lambda) + \beta_m(\lambda), \tag{2}$$

$\alpha_a(\lambda)$, $\alpha_m(\lambda)$ represent the absorption coefficient of the atmospheric aerosols and atmospheric molecule, $\beta_a(\lambda)$ and $\beta_m(\lambda)$ represent the scattering coefficient of the atmospheric aerosols and atmospheric molecule.

3.3. Channel model

UVC has two channel models: LOS model and NLOS model. The pointing angles of the transmitter and receiver in the LOS model require rigorous regulations to ensure that they are on the same horizontal line. The LOS model is suitable for point-to-point communication at a relatively short distance without obstacles between the transmitter side and receiver side. Path loss in the LOS model mainly derives from atmosphere absorption and scattering.

The LOS model is shown in Fig. 4(a). T_X represents the transmitter side, R_X represents the receiver side, Φ_1 is the transmitter's beam divergence angle and Φ_2 is the receiver's field-of-view (FOV). Assuming the transmitted power is P_t, $\frac{P_t e^{-K_e r_1}}{r_1^2}$ represents the transmitted power after a transmission distance of r_1. According to the Lambert–Beer law, after transmission distance of r_2, transmitted power further drops to $\frac{P_t e^{-K_e r_1}}{r_1^2} \times \left(\frac{\lambda}{4\pi r_2}\right)^2$.

The received power is:

$$P_{r,LOS} = P_t \left(\frac{e^{-K_e r_1}}{r_1^2}\right)\left(\frac{\lambda}{4\pi r_2}\right)^2 e^{-K_e r_2} = \frac{P_t A_r}{4\pi r_1^2 r_2^2} e^{-K_e(r_1+r_2)}. \tag{3}$$

Here, $e^{-K_e r_2}$ is the atmospheric attenuation coefficient, K_e is the extinction coefficient, λ is the wavelength of ultraviolet light, A_r is the receiver aperture area.

According to the geometric relationship in Fig. 4(a),

$$h_1 = \frac{r\sin(\Phi_2/2)}{\sin(\Phi_1/2 + \Phi_2/2)}, \tag{4}$$

$$h_2 = \frac{r\sin(\Phi_1/2)}{\sin(\Phi_1/2 + \Phi_2/2)}, \tag{5}$$

$$r_1 = h_1\cos(\Phi_1/2) = \frac{r\sin(\Phi_2/2)\cos(\Phi_1/2)}{\sin(\Phi_1/2 + \Phi_2/2)}, \tag{6}$$

$$r_2 = h_2\cos(\Phi_2/2) = \frac{r\sin(\Phi_1/2)\cos(\Phi_2/2)}{\sin(\Phi_1/2 + \Phi_2/2)}. \tag{7}$$

The received power can be further simplified into:

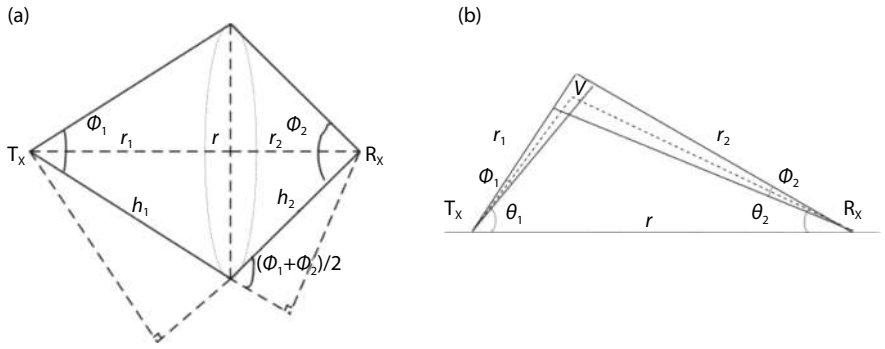

Fig. 4. Typical channel models of UVC: (a) LOS model, (b) NLOS model.

$$P_{r,LOS}=\frac{P_tA_r}{4\pi\left(\frac{r\sin(\Phi_2/2)\cos(\Phi_1/2)}{\sin(\Phi_1/2+\Phi_2/2)}\right)^2\left(\frac{r\sin(\Phi_1/2)\cos(\Phi_2/2)}{\sin(\Phi_1/2+\Phi_2/2)}\right)^2}e^{-K_e(r_1+r_2)}, \tag{8}$$

$$P_{r,LOS}=\frac{P_tA_r(\Phi_1/2+\Phi_2/2)}{4\pi r^4\sin^2(\Phi_2/2)\cos^2(\Phi_1/2)\sin^2(\Phi_1/2)\cos^2(\Phi_2/2)}e^{-K_e(r_1+r_2)}, \tag{9}$$

$$P_{r,LOS}=\frac{4P_tA_r}{\pi r^4}\frac{\sin^4(\Phi_1/2+\Phi_2/2)}{\sin^2\Phi_1\sin^2\Phi_2}e^{-K_er}. \tag{10}$$

According to Eq. (10), the received power is affected by the transmission distance r, the divergence angle of the light source Φ_1 and the reception angle of the detector Φ_2, the atmospheric attenuation coefficient e^{-K_er} and the reception gain of the detector $\frac{4\pi A_r}{\lambda^2}$. It can be seen that transmitted power drops exponentially with transmission distance in the LOS model, making UVC unfit for long-range communication.

In the NLOS model, the beam divergence angle of the transmitter and the FOV of the receiver are not directly pointing at each other. There are obstacles between the transmitter and receiver. In this case, the light signal can be received by detectors after multiple atmospheric scattering. A diagram of the NLOS model is shown in Fig. 4(b). Φ_1 is the transmitter's beam divergence angle, Φ_2 is the receiver's field-of-view (FOV), θ_1 and θ_2 are the elevation angle of transmitter and receiver. Assuming that P_t is transmitted power, $\frac{P_t}{\Omega_1}$ is the transmitted power per unit of stereo angle, $\frac{P_t}{\Omega_1}\frac{e^{-K_er_1}}{r_1^2}$ is the transmitted power after a transmission distance of r_1. Assuming the overlap between r_1 and r_2 is a secondary source composed of a large number of particles, and the output power of the secondary source is $\frac{P_t}{\Omega_1}\frac{e^{-K_er_1}}{r_1^2}\times\frac{K_sP_sV}{4\pi}$. The secondary source and receiver can be seen as a LOS model. The received power is expressed as:

$$P_{r,NLOS}=\frac{P_t}{\Omega_1}\frac{e^{-K_er_1}}{r_1^2}\times\frac{K_sP_sV}{4\pi}\left(\frac{\lambda}{4\pi r_2}\right)^2e^{-K_er_2}\frac{4\pi A_r}{\lambda^2}. \tag{11}$$

$\left(\frac{\lambda}{4\pi r_2}\right)^2$ is the free space path loss coefficient, $e^{-K_er_2}$ is the atmospheric attenuation coefficient, $\frac{4\pi A_r}{\lambda^2}$ is the receiver gain. According to the geometric relationship in Fig. 4(b),

$$\Omega_1=2\pi\left[1-\cos(\phi_1/2)\right], \tag{12}$$

$$r_1=r\sin\theta_2/\sin\theta_s, \tag{13}$$

$$r_2=r\sin\theta_1/\sin\theta_s, \tag{14}$$

$$\theta_s=\theta_1+\theta_2,\ V\gg r_2\phi_2d^2. \tag{15}$$

The final received power of the NLOS model can be simplified as

$$P_{r,NLOS}=\frac{P_tA_rK_sP_r\phi_2\phi_1^2\sin(\theta_1+\theta_2)}{32\pi^3r\sin\theta_1}\times\left(-\frac{K_er(\sin\theta_1+\sin\theta_2)}{\sin(\theta_1+\theta_2)}\right), \tag{16}$$

r is the distance between transmitter and receiver, K_e is the extinction coefficient, $K_e=K_s+K_a$, K_s is the scattering coefficient, K_a is the absorption coefficient. λ is the wavelength of ultraviolet light, A_r is the receiver aperture area, Ω_1 is the transmitter's stereo angle, V is the effective scattering volume, and P_s is the phase function of scattering angle of θ_s. A more detailed deduction can be found in Ref. [40].

3.4. Modulation

In UVC, light signals can be easily interfered by the background light noise during the propagation. Signals need to be superimposed on light waves which act as carrier waves to improve the stability and reliability of UVC. The intensity, frequency, phase, polarization of the carrier waves are modulated by the signals. The light signals that reach the photodetector will be demodulated to restore the original signal after opto-electrical (O-E) conversion.

Some of the most prevailing modulation schemes include OOK, pulse position modulation (PPM), fixed-length digital pulse interval modulation (FDPIM) and digital pulse interval modulation (DPIM). Different modulation schemes vary in terms of power utilization rate, frequency band utilization rate, channel capacity and inter-symbol interference. As the most used intensity modulation / direct detection (IM/DD) modulation scheme, OOK has the highest frequency band utilization rate and lowest inter-symbol interference, but its power utilization rate is the lowest among these four modulation schemes. Besides, OOK is easy to implement with no complex modulator circuits required. PPM has the highest frequency band utilization rate, making it suitable for long-range and high background noise UVC systems.

4. Light sources of UVC

UV light source is one of the most critical components of the UVC system. Its optical power essentially determines trans-

Table 1. Comparison of DUV light sources in UVC system.

Sources	Power	Wavelength (nm)	Lifetime (h)	Efficiency	Frequency	Ref.
Low-pressure mercury lamps	~kW	253.7	~16 000	~30%	~ kHz	[41]
High-pressure mercury lamps	~kW	253.7–366.3	~15 000	~17%	~ kHz	[42, 43]
KrF excimer laser	~W	248	~500	~4%	~Hz	[44]
Nd:YAG laser	~W	266	~1000	~8%	~Hz	[44]
UV LED	~mW	210–360	~15 000	~3%	~MHz	[45]

mission distance of UVC, while its bandwidth has a major impact on the data rate. As for the wavelength, shorter-wavelength signal will be less affected by the background noise, enabling a higher SNR for UVC. Gas discharge lamps, lasers and LEDs are the three most used light sources in the UVC system. Gas discharge lamps have great advantages in cost and output power. However, lasers excel in their high coherence, high monochromaticity and low divergence. They both share the same deficiency of heavy volume, large power consumption and low modulation rate. AlGaN-based LED has gained more and more attention in UVC due to its higher modulation rate and smaller chip size. By packaging multiple LED chips into one source array, its output power can reach up to Watt range. When reducing its size to the micrometer range, its bandwidth can reach up to GHz level[34]. A detailed comparison of DUV light sources in the UVC system is shown in Table 1.

4.1. DUV gas discharge lamp

As the first-used light source, the gas discharge lamp has a long history in UVC. Some of the most used UV gas discharge lamps include high and low-pressure mercury lamps, UV halide lamps and mercury xenon lamps. The conversion efficiency of the low-pressure mercury lamp can reach up to 30%–40%. In 1976, hydrogen-xenon arc lamps with high pulse repetition rates were used in the investigation of ultraviolet voice communication by Fishburne *et al.*[46]. They did a variety of communication tests during daylight hours, early evening hours and thunderstorms. High-quality voice communication is reported regardless of weather or time of day. Myer Geller and GB Johnson of Naval Ocean Systems Centre used two 25 W mercury discharge lamps filled with argon gas as light sources, achieving 2.4 Kb/s of data rate in both LOS and NLOS modes[47]. Under the average ozone concentration, the maximum transmission distance in LOS mode can reach 3 km, and the transmission distance in NLOS can reach 1 km. In 1990, Puschell *et al.* used mercury arc lamps with a modulation rate of 40 kHz and a peak wavelength of 265 nm as sources, achieved a high data rate (1.2 Mb/s) within the range of over 7 km[48].

4.2. DUV laser

Although gas discharge lamps have great advantages in output power, it still suffers from fragility and short lifetime. People begin to turn to other solar-blind sources like DUV laser. In 2010, an experimental test-bed using a narrow-pulsed ultraviolet (UV) laser was set up to characterize pulse broadening effects in short-range NLOS UVC channels by Chen *et al.*[49]. Wang *et al.* built a real-time UVC system using a 200 mW solid-state 266 nm laser as the light source in 2017[50]. A data rate of 400 Kb/s was measured with a frame error rate lower than 10^{-5}. Liao *et al.* experimentally and theoretically investigated long-distance NLOS UVC channel using a compact Q-switched fourth-harmonic neodymium-doped yttrium aluminum garnet (ND:YAG) 266 nm laser[51]. Sun *et al.* demonstrated an NLOS Underwater wireless optical communication (UWOC) link using a UV 375 nm laser diode[32, 33]. The schematic of the experimental setup for UV laser-based NLOS UWOC is shown in Fig. 5.

4.3. DUV LED

4.3.1. Introduction to DUV LED

As a pollution-free, low cost and high-efficiency optoelectronic device, AlGaN-based LEDs are replacing conventional mercury lamps as DUV light sources in many applications like sterilization, curing and medical diagnostics[52–55]. With recent advancements in DUV LEDs, the data rate and transmission range of LED-based UVC have reached an unprecedented level. More and more research groups have chosen DUV LEDs over DUV lasers or DUV gas lamps as the light sources for UVC due to its higher modulation rate and smaller chip size. However, AlGaN-based LEDs still suffer from relatively low output power and low quantum efficiency due to the high aluminum content[56]. The higher aluminum content theoretically enables a shorter emission wavelength, while also degrading the crystal quality due to the large thermal and lattice mismatch between substrate and epilayer. The increase of aluminum concentration will further enhance the activation energy of Mg in p-type AlGaN, which makes it challenging to obtain high hole concentration[56–58].

As the most ideal light source for UVC, the emission wavelength of AlGaN-based LEDs can be tuned from 210 to 360 nm which covers the entire solar-blind spectrum. Besides, LEDs exceed other light sources in bandwidth and response speed as well, facilitating its application in optical communication[59]. Table 2 summarizes the recent progress in UVC using DUV LEDs as the light source.

Sun *et al.* demonstrated a UVB-LED-based communication channel with a high data rate of 71 Mb/s. The proposed LED had an output power of 190 μW at 7 V bias voltage, wavelength of 294 nm and a −3 dB bandwidth of 29 MHz, as plotted in Figs. 6(a) and 6(b)[64]. In 2020, Omar *et al.* demonstrated a record-breaking data rate of 2.4 Gb/s at a distance of 1 m using a 279 nm LED with bandwidth of 170 MHz[60]. The experiment setup and the modulation bandwidth of the system are shown in Figs. 6(c) and 6(d). Yang *et al.* reported a solar-blind UV LED real-time video transmission system using a 265 nm LED as the source. The experimental results showed that the maximum data rate is 2.88 Mb/s and when the transmission distance was 4 m, the data rate can be up to 1.92 Mb/s. Sun *et al.* proposed and demonstrated a high data rate UVC system based on a 266 nm UV LED array with 50 mW luminous power[31]. The emitting source was driven by a three outputs constant-current control circuit, whose driving speed was up to 2 Mb/s.

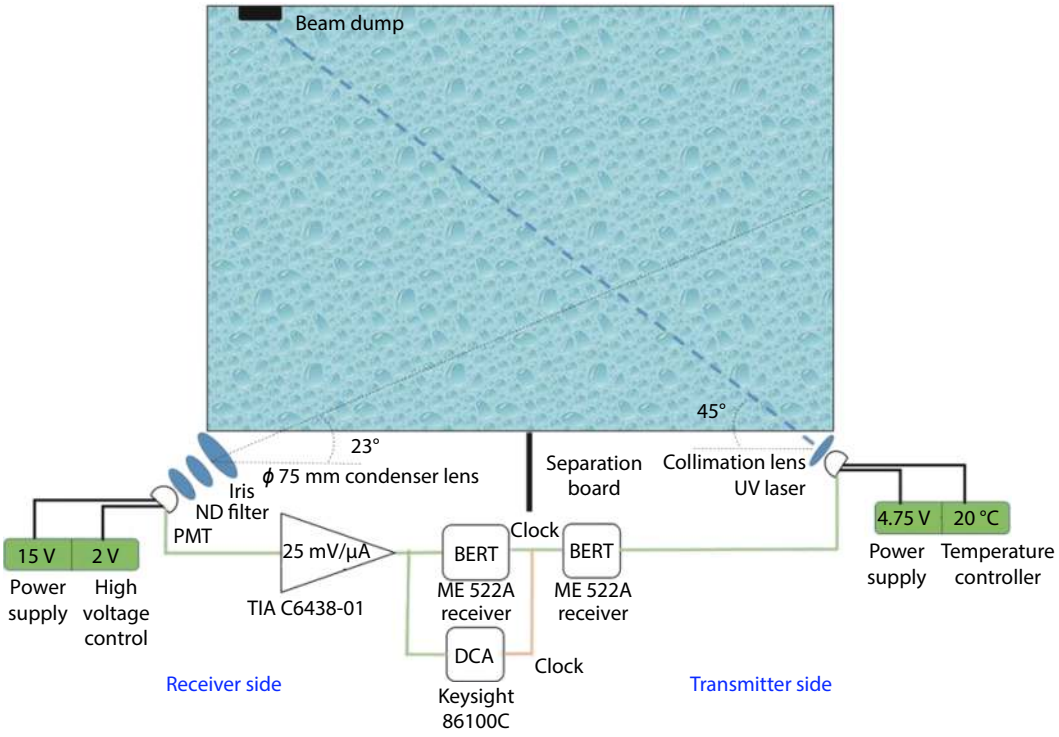

Fig. 5. (Color online) The schematic of the experimental setup for UV laser-based NLOS UWOC[33].

Table 2. Recent progress in UVC using LED as the light source.

Year	Light source	Detector	Wavelength (nm)	Bandwidth (MHz)	Modulation scheme	Max Range (m)	Speed	Ref.
2020	LED	Si APD	279	170	PAM-16	1	2.4 Gb/s	[60]
2020	LED	Si APD	279	170	PAM-16	5	1.09 Gb/s	[61]
2019	LED	Si APD	280	153		1.5	1.18 Gb/s	[62]
2018	LED	Si APD	280	153	PAM-4	1.6	1.6 Gb/s	[35]
2018	uLED	Si APD	262	438	OFDM	0.3	1 Gb/s	[34]
2018	LED	PMT	266	1.9		150	921.6 Kb/s	[31]
2018	LED	PIN	265		OOK		1.92 Mb/s	[63]
2017	LED	Si APD	294	29			71 Mb/s	[64]
2017	LED	PMT	260		OOK/PPM	100		[65]
2016	LED	PMT	265			40	250 Kb/s	[66]
2016	LED	PMT	260			100	64 Kb/s	[67]
2016	LED	PMT	265			20		[19]
2015	LED	PMT	265		OOK	35	64 Kb/s	[30]
2015	LED	PMT	265			20	64 Kb/s	[29]
2014	LED	PMT	265		OOK	20	8 Kb/s	[68]
2010	LED	PMT/APD	250		OOK/PPM		2 Mb/s	[69]
2008	LED	PMT	255		OOK			[70]
2008	LED	Si APD	250			170	100 Mb/s	[18]
2007	LED	PMT	271			106		[12]

4.3.2. Approaches to improve DUV LED bandwidth

Generally, the bandwidth of LEDs is affected by two factors: RC time constant[71, 72] and carrier lifetime[73, 74]. The RC time constant is determined by the device's resistance and capacitance, both of which can be tuned by the device size. Devices with larger sizes have lower bandwidth under the same current density. This is due to the reason that the increase in capacitance has a more significant impact on bandwidth than the decrease in resistance. By increasing carrier concentration, the radiative recombination rate will increase too, which leads to shorter carrier lifetime and more photons generating in the unit time. The bandwidth of LEDs eventually depends on the trade-off between these two factors. For conventional size LED under small current density, DUV LED bandwidth is dominated by carrier lifetime. As the current density increases, the carrier density in the multiple quantum wells (MQWs) increases too, leading to a shorter lifetime. As shown in Fig. 7(a), the modulation bandwidth at 40 mA is roughly threefold that of 20 mA[75]. But when the current density increases to a certain level, the carrier lifetime of DUV LED will saturate. Then RC time will have a major impact on the further decrease of carrier lifetime[76].

As a recent research hotspot, micro-LED shows great potential in high-speed optical communication[74, 77, 78]. Its

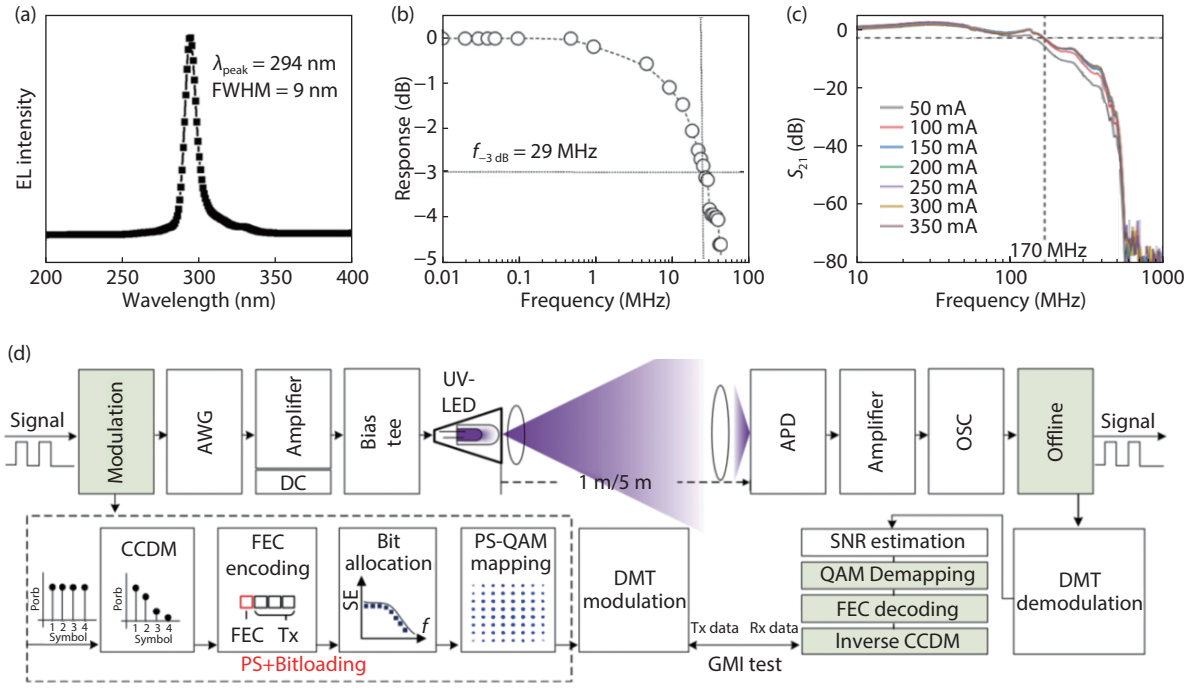

Fig. 6. (Color online) (a) Optical spectra of the LED under a bias voltage of 7 V[64]. (b) The small-signal frequency response of the system. The dashed line indicates the –3 dB bandwidth, which is approximately 29 MHz at distance = 0[64]. (c) The modulation bandwidth of the system at a distance of 5 m with different injection currents[60]. (d) The experimental setup and the flow diagram of the signal generation and offline processing[60].

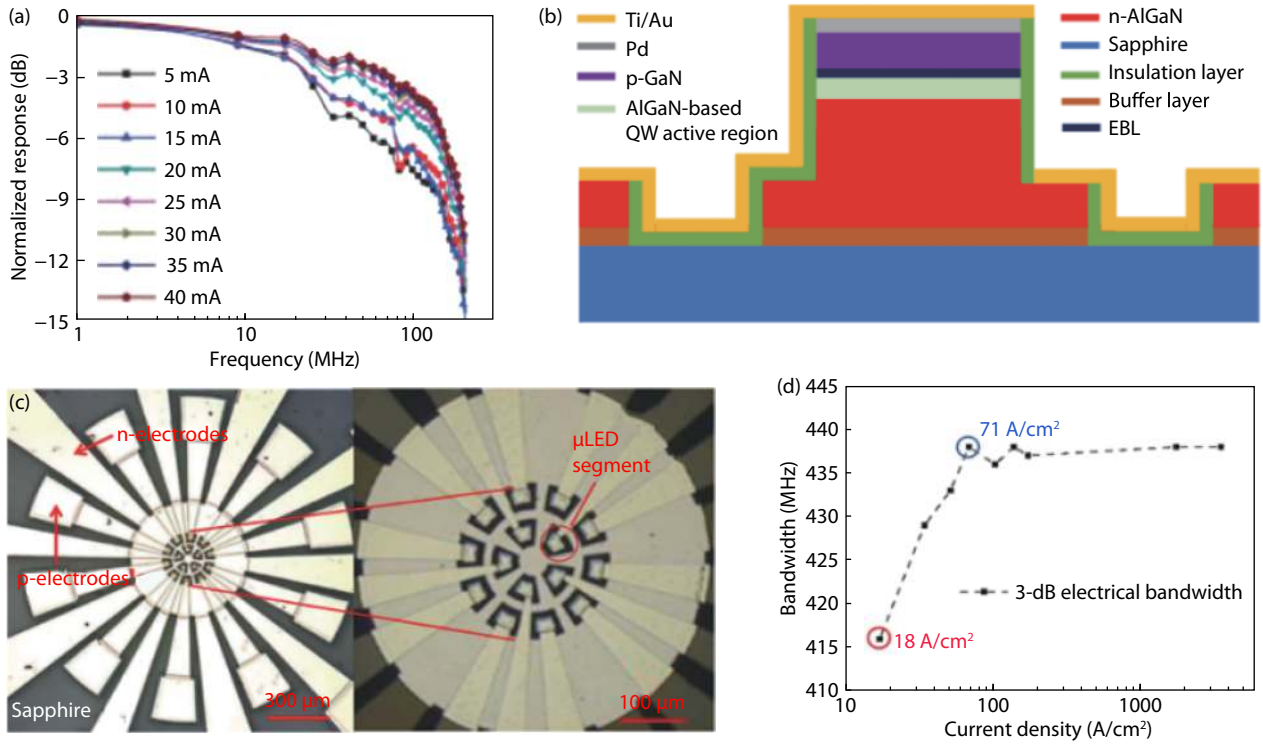

Fig. 7. (Color online) (a) A 4 × 4 matrix device structure with a single device size of 60 μm, with the corresponding changes in device response frequency and current[75]. (b) Simplified cross-sectional schematic of a single DUV μLED presented in this work. Dimensions are not to scale[34]. (c) Plan view optical image of the fabricated DUV μLED array presented in this work[34]. (d) The 3 dB electrical modulation bandwidth of the DUV μLED as a function of current density[34].

device size can be reduced to as small as 3.6 μm[79], and its bandwidth can reach up to 1.5 GHz[80]. Moreover, smaller chip size leads to better heat distribution and uniform current injection which results in a greater than two-fold decrease in the thermal resistance of the device, as compared with the conventional size LED[81]. AlGaN-based DUV micro-LED was first reported by Zhang *et al.* in 2003[82]. Since then, a lot of effort has been devoted to improving its output

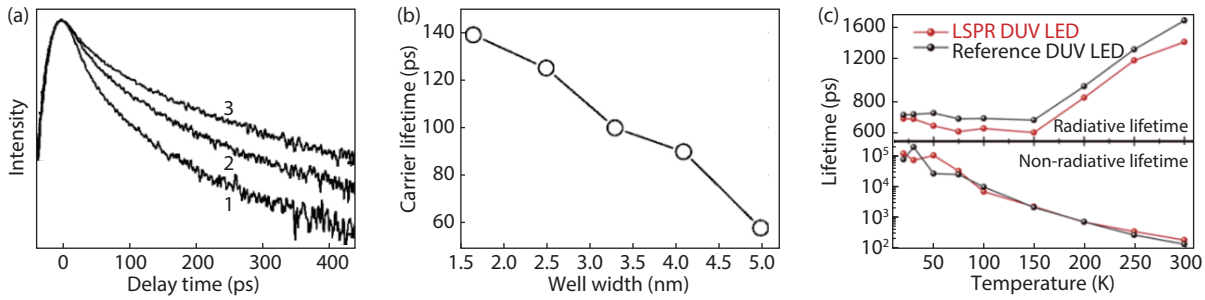

Fig. 8. (a) Normalized PL decay kinetics for AlGaN MQW structures with different well widths: (1) 5 nm, (2) 4.1 nm, and (3) 2.5 nm. Measurements were performed under excitation energy density of 25 mJ/cm^2[90]. (b) Well-width dependence of carrier lifetimes for AlGaN MQW structures at excitation energy density of 70 μJ/cm^2[90]. (c) Lifetime for different temperatures derived from the TD-TRPL results[91].

power and external quantum efficiency (EQE)[82–88]. In 2019, researchers from the UK first proposed 262 nm micro-LED as the light source for UVC[34]. Simplified cross-sectional schematic of a single DUV micro-LED and plan view optical image of the fabricated DUV μLED array were shown in Figs. 7(b) and 7(c). The measured 3 dB modulation bandwidth of these μLEDs initially increased linearly with the driving current density and then saturated as 438 MHz at a current density of 71 A/cm^2 as shown in Fig. 7(d), which was limited by the cutoff frequency of the commercial APD used for the measurement.

Carrier lifetime can also be effectively reduced by optimizing the MQW structure. LEDs with a thinner QW show a higher carrier density in the individual QW and a smaller spatial separation of the electron and hole wave functions by quantum-confined stark effect (QCSE)[89]. As the width of the quantum well increases, the radiative recombination rate and the optical power also increase. Time-resolved photoluminescence (TRPL) measurement of MQW with different well width of 2.5, 4.1 and 5 nm were depicted in Fig. 8(a)[90]. The carrier lifetime showed an inverse proportion to well width (Fig. 8(b)).

Quantum barrier height in MQW is modulated by its aluminum composition, which will further impact the radiative recombination rate and output power of DUV LEDs[92, 93]. LEDs with Al mole fraction of 55%, 60%, 67% and 76% in the QB were experimentally and numerically investigated by Guttmann *et al.* in Ref. [94]. When increasing the aluminum composition, the quantum barrier's binding effect on electrons and holes is enhanced, and the overlap between electron and hole wave function is increased. But when further increasing the height of the potential barrier, the MQW layers will act as a barrier to hole injection from the p-type layer, making the hole concentration and carrier lifetime in the quantum well decrease.

In 2017, Tian *et al.* investigated the impact of Si-doped AlGaN quantum barriers on the hole distribution in the MQWs, the radiative recombination rate and the optical powers of AlGaN DUV LED[95]. Results indicated that the Si-doped quantum barriers can significantly reduce the polarization induced electric field and increase the spatial overlap between the electron and hole wave functions in DUV LEDs. The device with Si doping concentration of 1×10^{19} cm^{-3} in quantum barriers showed a three-times increase in radiative recombination rate compared to the undoped ones.

Surface plasmon (SPs) can change the optical environment of the emitter due to its near-field enhancement properties. When the LED's MQW is coupled with SPs, a new energy conversion channel is added to the electron-hole pair. Thus, the energy of the electron-hole pair can be directly transferred to the SP, increasing the spontaneous radiative rate and reducing the carrier lifetime[91, 96–98]. By fabricating high-density and uniform Al nano-particles near the MQW active region, the IQE of AlGaN DUV LED showed a 57.7% enhancement with reduced radiative recombination lifetime from 1.71 to 1.40 ns as shown in Fig. 8(c)[91].

The electron blocking layer (EBL) between the p-type layer and active region in AlGaN-based LED can block the electrons overflowing from the active region and increase carrier residence time in MQW. However, EBL will also prevent the hole in the p-type layer from entering the active region. Numerical and experimental results indicate that LED with low barrier height EBL shows higher radiative recombination rate and hole injection efficiency, thereby leading to higher modulation bandwidth[99].

5. Detectors of UVC

As the most crucial components in the receiver side of UVC, detectors have a major impact on the BER and SNR of UVC. PMT is one of the most used PDs in scientific research due to their superior sensitivity and responsivity, especially in the detection of ultrashort pulse light and ultra-weak photons. Compared to the PIN and APD, PMT has a larger detection area, lower dark current and higher multiplication gains. But it is also fragile, expensive, and requires expensive solar-blind filters that fail to meet the trends of miniaturization for UVC. Besides, its bandwidth is merely 50 MHz, much lower than the commonly used Si-based detectors and SiC-base detectors. Semiconductor detectors like PINs and APDs still suffer from relatively high dark current and noise, which is about 5–6 orders of magnitude higher than PMT. APDs work under a much higher reverse bias than PDs, which increases the current gain to the order of 1000[100]. A detailed comparison is shown in Table 3.

5.1. PMTs

PMT has a long history in UVC, which is also the most used detectors since UVC is first put forward. Xing *et al.* studied the 2 × 2 MIMO scheme for UVC using two independent PMTs as the detectors, which have a 3 dB bandwidth of 5 MHz[66]. Narrowband interference UV filters are mounted on PMTs to block the ambient light as shown in Fig. 9(a). Raptis *et al.* studied the power losses in diffuse UVC channels[19].

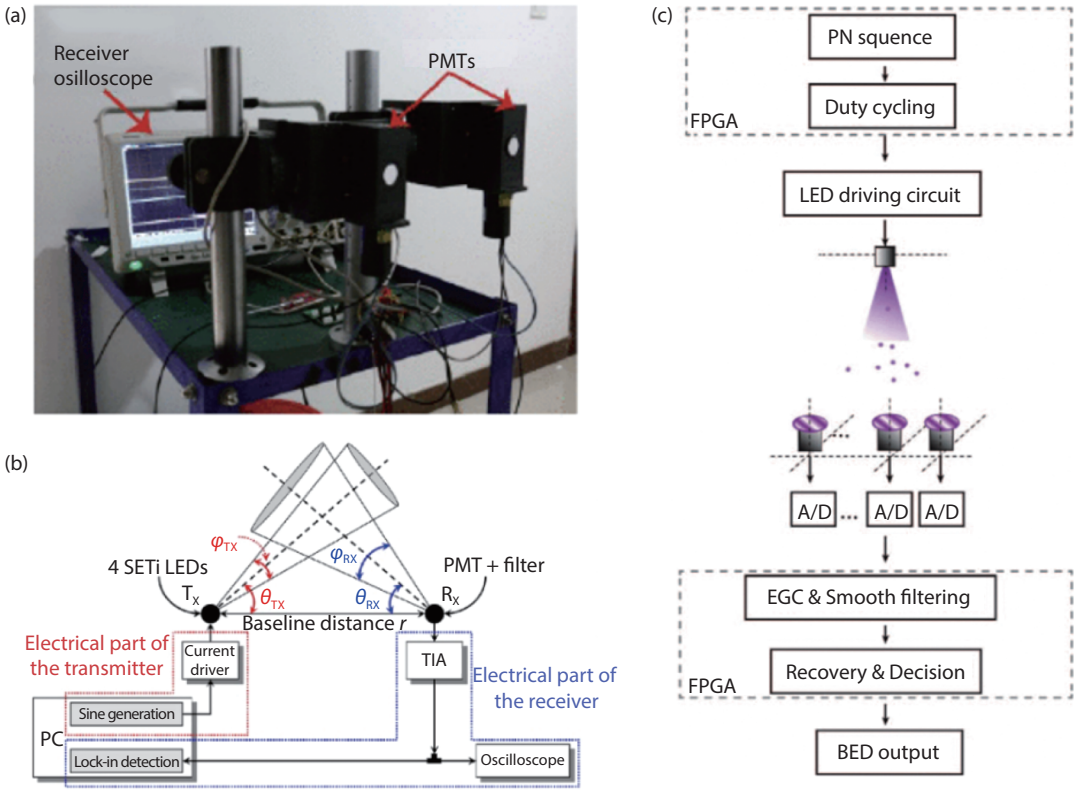

Fig. 9. (Color online) (a) The experimental setup of the receiver side[66]. (b) The experimental setup[19]. (c) Experimental setup for solar-blind NLOS UV communication with diversity reception[30].

Table 3. Comparison of DUV detectors in UVC system.

Detector	Spectral range (nm)	Responsivity (A/W)	Response time (ns)	Dark current (nA)	Ref
PMT	110–1100	~10^5	1–15	2–30	[101]
SiC PIN	200–400	0.085–0.13	~10	3×10^{-8}	
Si PIN	200–1100	~0.38	6–50	~10	
AlGaN PIN	220–280	~0.15	~6.5		[102]
Si APD	260–1100	0.24–0.5	~3×10^6	1–100	

The receiver consisted of a PMT (with a responsivity of 0.06 A/W at 265 nm). A large set of measurements at distances up to 20 m, for different elevation angles of the transmitter (UV-LEDs) and receiver (PMT) and for different atmospheric conditions have been taken for the characterization of the UVC channel in terms of path loss. The experiment setup is shown in Fig. 9(b). Meng *et al.* built up a four-receiver real-time platform and explored the characteristics and effectiveness of diversity reception in single-input-multiple-output (SIMO) UVC system with a four-PMT-detector array[30]. Each pair of PMTs was transversely separated by 150 mm as shown in Fig. 9(c). The experimental results for 1 × 4 SIMO UVC system showed that with a smaller Tx elevation or shorter distance, equal gain combining (EGC) may produce a diversity gain in the UV channel and thus improve the BER performance at low transmitter power.

5.2. Semiconductor PDs

Recently, the commercially available Si and SiC-based PINs and APDs have been replacing PMT in more and more scenarios. SiC-based PD shows excellent UV responsivity characteristics and a very low dark current between 200 and 400 nm. The responsivity at 270 nm is between 150 and 175 mA/W with a quantum efficiency of between 70% and 85%[103]. Several groups have reported UVC links using Si APD for UV detection[34, 64]. The reported detector has a wavelength range of 200–1000 nm, bandwidth of 400 MHz, responsivity of 15 A/W and an active area diameter of 0.2 mm. Kojima *et al.* used a 1 GHz Si-based APD with 30 kV/W responsibility at 250 nm in UVC link[35, 62].

AlGaN-based APDs are intrinsically solar-blind with no additional filters required and are an ideal alternative to current bulky and fragile PMTs. In 2014, Shao *et al.* reported an AlGaN-based APD with a record-high gain of 1.2×10^4 and a peak responsivity of 0.15 A/W around 280 nm[104]. The absorption and multiplication zone were separated by a 60 nm n-type $Al_{0.4}Ga_{0.6}N$ layer and thus yielded higher gain and lower noise than the regular APD.

5.3. Potential detectors for UVC

Recently, solar-blind detectors with novel material and device structure have been proposed extensively, among which Ga_2O_3, ZnO-Ga_2O_3 and MgZnO based detectors have shown great potential in replacing the current solar-blind detectors for UVC. With its wide bandgap of 4.9 eV, Ga_2O_3-based PDs are perfectly fit for solar-blind detection in UVC[105–107]. Hu *et al.* fabricated Au-Ga_2O_3-Au based solar-

blind PDs which showed a maximum responsivity at around 255 nm and a cutoff wavelength of 260 nm[108]. solar-blind PDs based on Ga_2O_3/SnO_2 and Ga_2O_3/Si heterostructures were also reported by Mahmoud and Guo in 2016[109, 110].

The lattice mismatch between ZnO and Ga_2O_3 is relatively small, making it easier to grow Ga_2O_3 on ZnO. And the large conduction band offsets between Ga_2O_3 and ZnO prompt large avalanche multiplication which leads to larger responsivity. Zhao *et al.* proposed a single core-shell microwire APDs based on ZnO–Ga_2O_3 heterostructure[111]. The proposed APDs with peak responsivity of 1.3×10^3 A/W, detectivity of 9.91×10^{14} cm·Hz$^{1/2}$/W and response time of 20 μs under −6 V bias exhibited excellent photo-response performances compared to commercial Si-based APDs.

MgZnO is another promising candidate for solar-blind PDs. Theoretically, the bandgap of MgZnO can be tuned from 3.4 to 7.8 eV by changing the Mg content. But the fabrication technique for MgZnO is still in its infancy due to the large mismatch between the MgZnO epilayer and its common substrates. Du *et al.* first proposed MgZnO-based solar-blind PDs in 2009[112]. Since then, more and more groups have participated in this area. In 2016, Alema *et al.* achieved a record high responsivity of ~1.8×10^4 A/W at 276 nm under 10 V bias for MgZnO-based solar-blind PDs[113]. This is attributed to the asymmetric barrier height at the two sides of the MSM (metal–semiconductor–metal) electrodes which gave rise to the carrier trapping states at the MgZnO/Ni/Au interface.

6. Future application of UVC

UVC has a lot of potential applications in underwater communication, vehicular communication and machine-to-machine communication. The frequency band used in UVC is much higher than that of radio frequency (RF) communication, so traditional electromagnetic interference (EMI) technology and signal interception technology cannot be applied to UVC, guarenteeing confidential and interference-free communication environment for UVC. We present some scenarios where UVC can be a viable alternative to conventional communication.

6.1. Battlefield applications

On the battlefield, radio sometimes needs to be turned off to conceal operation. Under this circumstance, gestures or code words will usually be used for short-range communication. By using UVC as the alternative, unicast, multicast and broadcast communications will be possible. Short-range communication in conventional tactical operations usually requires cable, but the cable set-up requires extra time severely restraining the speed and maneuverability of operation. While UVC systems can be quickly set up with no cable required.

6.2. Aircraft guidance system

UVC can also be used in take-off guidance systems among control towers, aircraft carriers and aircraft[114]. Transmitters can be mounted on the bridge of the aircraft carrier to radiate UV light signals horizontally to the deck, and each aircraft is equipped with a small receiver to collect guidance signals distributed in the air. The light signal from the transmitters can illuminate the entire flight deck so that the aircraft can move freely and receive signals simultaneously.

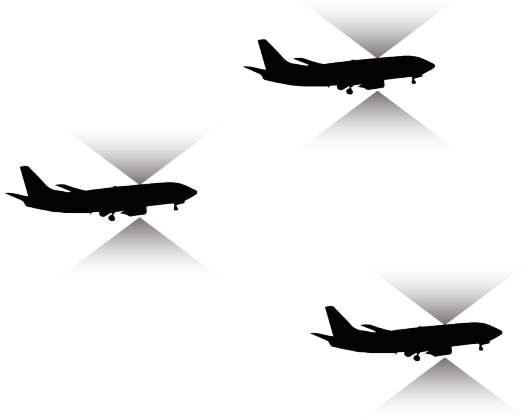

Fig. 10. Application of UVC in aircraft squad.

6.3. Aircraft squad communication

UVC systems can be used for confidential communications among aircraft squad as shown in Fig. 10. In this case, each aircraft is equipped with a transceiver system. The transmitter radiates light signals in a horizontal direction and the receiver is mounted facing the sky to collect UV signals scattered into its FOV to build electromagnetically silent and secure internal communications.

7. Conclusion and outlook of UVC

In this article, we summarize and describe the history and working principle of UVC. A comprehensive comparison of its light sources and detectors is provided to the best of our knowledge. Then we discuss the research progress of UVC from a device perspective. For light sources, our review is based on three of the most used UV light sources including gas discharge lamp, laser and LED. For detectors, other than the commonly used detectors including PMTs and semiconductor PDs, we also discuss some potential solar-blind detectors for UVC. Finally, we present the application and outlook of UVC. Hopefully, this review will offer valuable insights into the future development of UVC.

As a novel optical communication, UVC shows great potential in replacing conventional communication. Rich theory on the networking, channel model, modulation scheme and signal processing have been put forward and verified experimentally[4, 115, 116]. However, light sources and detectors still are the two bottlenecks restricting UVC's wide application. With high security, high stability, low power loss and short response time, AlGaN-based LEDs have been considered as one of the most ideal light sources for UVC[117, 118]. However, the research on its bandwidth is still in its infancy. How to improve the bandwidth of DUV LEDs in terms of material growth, device structure, manufacturing process and packaging is still an open question. PMT has gradually been replaced by its cheap and efficient counterparts like PINs and APDs in UVC. But solar-blind PINs and APDs still suffer from relatively high dark current and low responsivity. Improvement in fabrication techniques and device structures is expected to resolve these issues.

Acknowledgements

This work was financially supported by the National Key

R&D Program of China (No. 2019YFA0708203), the National Natural Science Foundation of China (No. 61974139), and the Beijing Natural Science Foundation (No. 4182063).

References

[1] Khalighi M A, Uysal M. Survey on free space optical communication: A communication theory perspective. IEEE Commun Surv Tutor, 2014, 16(4), 2231

[2] Rajbhandari S, McKendry J J, Herrnsdorf J, et al. A review of gallium nitride LEDs for multi-gigabit-per-second visible light data communications. Semicond Sci Technol, 2017, 32(2), 023001

[3] Shaw G A, Nischan M L, Iyengar M A, et al. NLOS UV communication for distributed sensor systems. International Symposium on Optical Science and Technology, 2000, 83

[4] Xu Z, Sadler B M. Ultraviolet communications: potential and state-of-the-art. IEEE Commun Mag, 2008, 46(5), 67

[5] Harvey G. A survey of ultraviolet communication systems. Washington: Naval Research Laboratory, 1964

[6] White H. Communication by non-visible ultraviolet radiation. Berkeley: University of California Press, 1945

[7] Sunstein D E. A scatter communications link at ultraviolet frequencies. PhD Dissertation, Massachusetts Institute of Technology, 1968

[8] Charles B, Hughes B, Erickson A, et al. Ultraviolet laser-based communication system for short-range tactical applications. OE/LASE '94, 1994, 79

[9] Shaw G A, Siegel A M, Model J, et al. Field testing and evaluation of a solar-blind UV communication link for unattended ground sensors. Defense and Security, 2004, 250

[10] Shaw G A, Siegel A M, Model J. Extending the range and performance of non-line-of-sight ultraviolet communication links. Defense and Security Symposium, 2006, 62310C

[11] Xu Z, Tsatsanis M K. Blind adaptive algorithms for minimum variance CDMA receivers. IEEE Trans Commun, 2001, 49(1), 180

[12] Xu Z, Chen G, Abou-Galala F, et al. Experimental performance evaluation of non-line-of-sight ultraviolet communication systems. Optical Engineering + Applications, 2007, 67090Y

[13] Xu Z, Ding H, Sadler B M, et al. Analytical performance study of solar blind non-line-of-sight ultraviolet short-range communication links. Opt Lett, 2008, 33(16), 1860

[14] Liu L D, Ni G Q, Zhong S D, et al. Application and detection of ultraviolet and their new development. Opt Technol, 1998, 2, 87 (in Chinese)

[15] Ni G Q. Study on ultraviolet communication through disengaged atmodphere. Opt Tech, 2000, 26, 297 (in Chinese)

[16] Tang Y, Ni G, Zhang L, et al. Study of single scatter model in NLOS UV communication. Opt Tech, 2007, 33, 759 (in Chinese)

[17] Tang Y, Wu Z L, Ni G Q, et al. NLOS single scattering model in digital UV communication. Asia-Pacific Opt Communi, 2008, 713615

[18] Kedar D, Arnon S. Subsea ultraviolet solar-blind broadband free-space optics communication. Opt Eng, 2009, 48(4), 046001

[19] Raptis N, Pikasis E, Syvridis D. Power losses in diffuse ultraviolet optical communications channels. Opt Lett, 2016, 41(18), 4421

[20] Yin H, Chang S, Wang X, et al. Analytical model of non-line-of-sight single-scatter propagation. J Opt Soc Am A, 2010, 27(7), 1505

[21] Yin H, Chang S, Jia H, et al. Non-line-of-sight multiscatter propagation model. J Opt Soc Am A, 2009, 26(11), 2466

[22] Zhang H, Yin H, Jia H, et al. Study of effects of obstacle on non-line-of-sight ultraviolet communication links. Opt Express, 2011, 19(22), 21216

[23] Zhang H. Study on the characteristics of propagation of ultraviolet communication system. PhD Dissertation, National University of Defense Technology, 2012 (in Chinese)

[24] Yin H, Yang J, Chang S, et al. Analysis of several factors influencing range of non-line-of-sight UV transmission. Asia-Pacific Optical Communications, 2007, 67833E

[25] Jia H, Huang H X, Zhang H. Influence factors on data speed of wireless ultraviolet communication. Optics & Optoelectronic Technology, 2010, 1, 20 (in Chinese)

[26] Zuo Y, Xiao H, Wu J, et al. A single-scatter path loss model for non-line-of-sight ultraviolet channels. Opt Express, 2012, 20(9), 10359

[27] Zuo Y, Wu Jian, Xiao H F, et al. Non-line-of-sight ultraviolet communication performance in atmospheric turbulence. China Commun, 2013, 10(11), 52

[28] Xiao H, Zuo Y, Wu J, et al. Non-line-of-sight ultraviolet single-scatter propagation model in random turbulent medium. Opt Lett, 2013, 38(17), 3366

[29] Guo L, Meng D, Liu K, et al. Experimental research on the MRC diversity reception algorithm for UV communication. Appl Opt, 2015, 54(16), 5050

[30] Meng X, Zhang M, Han D, et al. Experimental study on 1× 4 real-time SIMO diversity reception scheme for a ultraviolet communication system. European Conference on Networks and Optical Communications (NOC), 2015, 1

[31] Sun Z, Zhang L, Qin Y, et al. 1 Mbps NLOS solar-blind ultraviolet communication system based on UV-LED array. International Conference on Optical Instruments and Technology 2017, 2017, 106170O

[32] Sun X, Cai W, Alkhazragi O, et al. 375-nm ultraviolet-laser based non-line-of-sight underwater optical communication. Opt Express, 2018, 26(10), 12870

[33] Sun X, Kong M, Alkhazragi O, et al. Non-line-of-sight methodology for high-speed wireless optical communication in highly turbid water. Opt Commun, 2020, 461, 125264

[34] He X, Xie E, Islim M S, et al. 1 Gbps free-space deep-ultraviolet communications based on III-nitride micro-LEDs emitting at 262 nm. Photonics Res, 2019, 7(7), B41

[35] Kojima K, Yoshida Y, Shiraiwa M, et al. 1.6-Gbps LED-based ultraviolet communication at 280 nm in direct sunlight. 2018 European Conference on Optical Communication (ECOC), 2018, 1

[36] Laj P, Klausen J, Bilde M, et al. Measuring atmospheric composition change. Atmos Environ, 2009, 43(33), 5351

[37] Walter V, Saska M, Franchi A. Fast mutual relative localization of uavs using ultraviolet led markers. 2018 International Conference on Unmanned Aircraft Systems (ICUAS), 2018, 1217

[38] Andrews D L. Rayleigh scattering and Raman effect, theory. In: Encyclopedia of Spectroscopy and Spectrometry. Boston: Academic Press, 2016

[39] Swinehart D F. The beer-lambert law. J Chem Educ, 1962, 39(7), 333

[40] Luettgen M R, Shapiro J H, Reilly D M. Non-line-of-sight single-scatter propagation model. J Opt Soc Am A, 1991, 8(12), 1964

[41] Sholtes K A, Lowe K, Walters G W, et al. Comparison of ultraviolet light-emitting diodes and low-pressure mercury-arc lamps for disinfection of water. Environ Technol, 2016, 37(17), 2183

[42] Pousset T, Cussac P, Zissis G, et al. Electronic ballast for high-pressure mercury lamps. 1996 IEEE Industry Applications Society Annual Meeting, 1996, 2109

[43] Van Bommel W. Road lighting: Fundamentals, technology and application. Berlin: Springer, 2014

[44] Ready J F. Industrial applications of lasers. Amsterdam: Elsevier, 1997

[45] Sun K X, Leindecker N, Higuchi S, et al. UV LED operation lifetime and radiation hardness qualification for space flights. 7th International LISA Symposium, 2008, 012028

[46] Fishburne E, Neer M E, Sandri G. Voice communication via scattered ultraviolet radiation. New Jersey: Aeronautical Research Associates Of Princeton Inc, 1976
[47] Geller M, Keenan T E, Altman D E, et al. Optical non-line-of-sight covert, secure high data communication system. US Patents, US4493114, 1985
[48] Puschell J J, Bayse R. High data rate ultraviolet communication systems for the tactical battlefield. Tactical Communications Conference, 1990, 253
[49] Chen G, Xu Z, Sadler B M. Experimental demonstration of ultraviolet pulse broadening in short-range non-line-of-sight communication channels. Opt Express, 2010, 18(10), 10500
[50] Wang K, Gong C, Zou D, et al. Demonstration of a 400 kbps real-time non-line-of-sight laser-based ultraviolet communication system over 500 m. Chin Opt Lett, 2017, 15(4), 040602
[51] Liao L, Drost R J, Li Z, et al. Long-distance non-line-of-sight ultraviolet communication channel analysis: experimentation and modelling. IET Optoelectron, 2015, 9(5), 223
[52] Würtele M, Kolbe T, Lipsz M, et al. Application of GaN-based ultraviolet-C light emitting diodes – UV LEDs – for water disinfection. Water Res, 2011, 45(3), 1481
[53] Siegel S B. Light emitting apparatus and method for curing inks, coatings and adhesives. US Patents, US7175712, 2007
[54] Hirayama H. Research status and prospects of deep ultraviolet devices. J Semicond, 2019, 40(12), 120301
[55] Barolet D. Light-emitting diodes (LEDs) in dermatology. Semin Cutan Med Surg, 2008, 27(4), 227
[56] Khan A, Balakrishnan K, Katona T. Ultraviolet light-emitting diodes based on group three nitrides. Nat Photonics, 2008, 2(2), 77
[57] Kneissl M, Kolbe T, Chua C, et al. Advances in group III-nitride-based deep UV light-emitting diode technology. Semicond Sci Technol, 2010, 26(1), 014036
[58] Li J, Ji G, Yang W, et al. Emission mechanism of high Al-content AlGaN multiple quantum wells. Chin J Lumin, 2016, 37(5), 513 (in Chinese)
[59] Komine T, Nakagawa M. Fundamental analysis for visible-light communication system using LED lights. IEEE Trans Consum Electron, 2004, 50(1), 100
[60] Alkhazragi O, Hu F, Zou P, et al. 2.4-Gbps ultraviolet-C solar-blind communication based on probabilistically shaped DMT modulation. 2020 Optical Fiber Communication Conference, 2020, M3I.5
[61] Alkhazragi O, Hu F, Zou P, et al. Gbit/s ultraviolet-C diffuse-line-of-sight communication based on probabilistically shaped DMT and diversity reception. Opt Express, 2020, 28(7), 9111
[62] Yoshida Y, Kojima K, Shiraiwa M, et al. An outdoor evaluation of 1-Gbps optical wireless communication using AlGaN-based LED in 280-nm band. 2019 Conference on Lasers and Electro-Optics (CLEO), 2019, 1
[63] Yang Y, Chen X H, You B, et al. Design of solar blind ultraviolet LED real-time video transmission system. Infrared Laser Eng, 2018, 47, 1022001 (in Chinese)
[64] Sun X, Zhang Z, Chaaban A, et al. 71-Mbit/s ultraviolet-B LED communication link based on 8-QAM-OFDM modulation. Opt Express, 2017, 25(19), 23267
[65] Qin H, Zuo Y, Li F, et al. Analytical link bandwidth model based square array reception for non-line-of-sight ultraviolet communication. Opt Express, 2017, 25(19), 22693
[66] Xing Y, Zhang M, Han D, et al. Experimental study of a 2 × 2 MIMO scheme for ultraviolet communications. 2016 15th International Conference on Optical Communications and Networks (ICOCN), 2016, 1
[67] Song P, Zhao T, Ke X, et al. Multi-user interference in a non-line-of-sight ultraviolet communication network. IET Commun, 2016, 10(13), 1640
[68] Zhang M, Luo P, Guo X, et al. Spread spectrum-based ultraviolet communication with experiments. Chin Opt Lett, 2014, 12(10), 100602
[69] He Q, Xu Z, Sadler B M. Performance of short-range non-line-of-sight LED-based ultraviolet communication receivers. Opt Express, 2010, 18(12), 12226
[70] Chen G, Abou-Galala F, Xu Z, et al. Experimental evaluation of LED-based solar blind NLOS communication links. Opt Express, 2008, 16(19), 15059
[71] Shi J W, Chen C C, Sheu J K, et al. Linear cascade GaN-based green light-emitting diodes with invariant high-speed/power performance under high-temperature operation. IEEE Photon Technol Lett, 2008, 20(23), 1896
[72] Shi J W, Sheu J K, Wang C K, et al. Linear cascade arrays of GaN-based green light-emitting diodes for high-speed and high-power performance. IEEE Photon Technol Lett, 2007, 19(18), 1368
[73] Shi J W, Sheu J K, Chen C H, et al. High-speed GaN-based green light-emitting diodes with partially n-doped active layers and current-confined apertures. IEEE Electron Device Lett, 2008, 29(2), 158
[74] McKendry J J, Green R P, Kelly A, et al. High-speed visible light communications using individual pixels in a micro light-emitting diode array. IEEE Photon Technol Lett, 2010, 22(18), 1346
[75] Huang Y, Guo Z, Huang H, et al. Influence of current density and capacitance on the bandwidth of VLC LED. IEEE Photon Technol Lett, 2018, 30(9), 773
[76] Zhu S C, Zhao L X, Yang C, et al. GaN-based flip-chip parallel micro LED array for visible light communication. 2017 International Conference on Optoelectronics and Microelectronics Technology and Application, 2016, 102441Y
[77] McKendry J J, Massoubre D, Zhang S, et al. Visible-light communications using a CMOS-controlled micro-light-emitting-diode array. J Light Technol, 2011, 30(1), 61
[78] Ferreira R X, Xie E, McKendry J J, et al. High bandwidth GaN-based micro-LEDs for multi-Gb/s visible light communications. IEEE Photon Technol Lett, 2016, 28(19), 2023
[79] Bai J, Cai Y, Feng P, et al. Ultra-small, ultra-compact and ultra-high efficient InGaN micro light emitting diodes (μLEDs) with narrow spectral linewidth. ACS Nano, 2020, 14(6), 6909
[80] Rashidi A, Monavarian M, Aragon A, et al. Nonpolar *m*-plane InGaN/GaN micro-scale light-emitting diode with 1.5 GHz modulation bandwidth. IEEE Electron Device Lett, 2018, 39(4), 520
[81] Ploch N L, Rodriguez H, Stolmacker C, et al. Effective thermal management in ultraviolet light-emitting diodes with micro-LED arrays. IEEE Trans Electron Devices, 2013, 60(2), 782
[82] Zhang J, Wu S, Rai S, et al. AlGaN multiple-quantum-well-based, deep ultraviolet light-emitting diodes with significantly reduced long-wave emission. Appl Phys Lett, 2003, 83(17), 3456
[83] Hwang S, Islam M, Zhang B, et al. A hybrid micro-pixel based deep ultraviolet light-emitting diode lamp. Appl Phys Express, 2010, 4(1), 012102
[84] Wu S, Chhajed S, Yan L, et al. Matrix addressable micro-pixel 280 nm deep UV light-emitting diodes. Jpn J Appl Phys, 2006, 45(4L), L352
[85] Adivarahan V, Wu S, Sun W, et al. High-power deep ultraviolet light-emitting diodes basedon a micro-pixel design. Appl Phys Lett, 2004, 85(10), 1838
[86] Adivarahan V, Heidari A, Zhang B, et al. 280 nm deep ultraviolet light emitting diode lamp with an AlGaN multiple quantum well active region. Appl Phys Express, 2009, 2(10), 102101
[87] Sun W, Adivarahan V, Shatalov M, et al. Continuous wave milliwatt power AlGaN light emitting diodes at 280 nm. Jpn J Appl Phys, 2004, 43(11A), L1419

[88] Wu S, Adivarahan V, Shatalov M, et al. Micro-pixel design milliwatt power 254 nm emission light emitting diodes. Jpn J Appl Phys, 2004, 43(8A), L1035
[89] Zhu S, Lin S, Li J, et al. Influence of quantum confined Stark effect and carrier localization effect on modulation bandwidth for GaN-based LEDs. Appl Phys Lett, 2017, 111(17), 171105
[90] Mickevičius J, Tamulaitis G, Kuokštis E, et al. Well-width-dependent carrier lifetime in AlGaN/AlGaN quantum wells. Appl Phys Lett, 2007, 90(13), 131907
[91] Lee J W, Ha G, Park J, et al. AlGaN deep-ultraviolet light-emitting diodes with localized surface plasmon resonance by a high-density array of 40 nm Al nanoparticles. ACS Appl Mater Interfaces, 2020, 12(32), 36339
[92] Wang C, Chiou Y, Hsiang C, et al. Enhancement of optical performance of near-UV nitride-based light emitting diodes with different aluminum composition barrier structure. Phys Status Solidi A, 2014, 211(8), 1769
[93] Kajitani R, Kawasaki K, Takeuchi M. Barrier-height and well-width dependence of photoluminescence from AlGaN-based quantum well structures for deep-UV emitters. Mater Sci Eng B, 2007, 139(2/3), 186
[94] Guttmann M, Höpfner J, Reich C, et al. Effect of quantum barrier composition on electro-optical properties of AlGaN-based UVC light emitting diodes. Semicond Sci Technol, 2019, 34(8), 085007
[95] Tian K, Chen Q, Chu C, et al. Investigations on AlGaN-based deep-ultraviolet light-emitting diodes with Si-doped quantum barriers of different doping concentrations. Phys Status Solidi RRL, 2018, 12(1), 1700346
[96] Guo W, Xu H, Yang Z, et al. Performance enhancement of ultraviolet light emitting diode incorporating Al nanohole arrays. Nanotechnology, 2018, 29(45), 45LT01
[97] Huang K, Gao N, Wang C, et al. Top-and bottom-emission-enhanced electroluminescence of deep-UV light-emitting diodes induced by localised surface plasmons. Sci Rep, 2014, 4(1), 4380
[98] Gao N, Huang K, Li J, et al. Surface-plasmon-enhanced deep-UV light emitting diodes based on AlGaN multi-quantum wells. Sci Rep, 2012, 2(1), 816
[99] Zhu S, Wang J, Yan J, et al. Influence of AlGaN electron blocking layer on modulation bandwidth of GaN-based light emitting diodes. ECS Solid State Lett, 2014, 3(3), R11
[100] Kharraz O, Forsyth D. Performance comparisons between PIN and APD photodetectors for use in optical communication systems. Optik, 2013, 124(13), 1493
[101] Photonics H. Photomultiplier tubes. Hamamatsu: Hamamatsu Photonics, 2000
[102] Chen Y, Zhang Z, Jiang H, et al. The optimized growth of AlN templates for back-illuminated AlGaN-based solar-blind ultraviolet photodetectors by MOCVD. J Mater Chem C, 2018, 6(18), 4936
[103] Brown D M, Downey E T, Ghezzo M, et al. Silicon carbide UV photodiodes. IEEE Trans Electron Devices, 1993, 40(2), 325
[104] Shao Z G, Chen D J, Lu H, et al. High-gain AlGaN solar-blind avalanche photodiodes. IEEE Electron Device Lett, 2014, 35(3), 372
[105] Higashiwaki M, Sasaki K, Murakami H, et al. Recent progress in Ga_2O_3 power devices. Semicond Sci Technol, 2016, 31(3), 034001
[106] Li W, Zhang X, Meng R, et al. Epitaxy of III-nitrides on β-Ga_2O_3 and its vertical structure LEDs. Micromachines, 2019, 10(5), 322
[107] Pearton S, Yang J, Cary IV P H, et al. A review of Ga_2O_3 materials, processing, and devices. Appl Phys Rev, 2018, 5(1), 011301
[108] Hu G, Shan C, Zhang N, et al. High gain Ga_2O_3 solar-blind photodetectors realized via a carrier multiplication process. Opt Express, 2015, 23(10), 13554
[109] Mahmoud W E. Solar blind avalanche photodetector based on the cation exchange growth of β-Ga_2O_3/SnO_2 bilayer heterostructure thin film. Sol Energy Mater Sol Cells, 2016, 152, 65
[110] Guo X, Hao N, Guo D, et al. β-Ga_2O_3/p-Si heterojunction solar-blind ultraviolet photodetector with enhanced photoelectric responsivity. J Alloys Compd, 2016, 660, 136
[111] Zhao B, Wang F, Chen H, et al. Solar-blind avalanche photodetector based on single ZnO–Ga_2O_3 core–shell microwire. Nano Lett, 2015, 15(6), 3988
[112] Du X, Mei Z, Liu Z, et al. Controlled growth of high-quality ZnO-based films and fabrication of visible-blind and solar-blind ultraviolet detectors. Adv Mater, 2009, 21(45), 4625
[113] Alema F, Hertog B, Ledyaev O, et al. High responsivity solar blind photodetector based on high Mg content MgZnO film grown via pulsed metal organic chemical vapor deposition. Sens Actuator A, 2016, 249, 263
[114] Lavigne C, Durand G, Roblin A. Ultraviolet light propagation under low visibility atmospheric conditions and its application to aircraft landing aid. Appl Opt, 2006, 45(36), 9140
[115] Yuan R, Ma J. Review of ultraviolet non-line-of-sight communication. China Commun, 2016, 13(6), 63
[116] Vavoulas A, Sandalidis H G, Chatzidiamantis N D, et al. A survey on ultraviolet C-band (UV-C) communications. IEEE Commun Surv Tutor, 2019, 21(3), 2111
[117] Razeghi M. Deep ultraviolet light-emitting diodes and photodetectors for UV communications. Integrated Optoelectronic Devices, 2005, 2005, 30
[118] Li J M, Liu Z, Liu Z Q, et al. Advances and prospects in nitrides based light-emitting-diodes. J Semicond, 2016, 37(6), 061001

Liang Guo is currently pursuing his M.S. degree in the Institute of Semiconductors, Chinese Academy of Sciences. He received his B.S. degree in Materials Physics from Hefei University of Technology in 2018. His research mainly focuses on the fabrication of deep-UV LEDs for communications.

Tongbo Wei is currently a professor in Institute of Semiconductors, Chinese Academy of Sciences. He received his doctoral degree in engineering from Chinese Academy of Sciences in July 2007. His research interests focus on wide bandgap semiconductor materials and devices, new micro-nano photoelectronic devices, deep ultraviolet light emitting devices, and nitride growth on two-dimensional materials.